JOURNAL OF GEOPHYSICAL RESEARCH, VOL. 102, NO. D22, PAGES 26,247–26,261, NOVEMBER 27, 1997

Estimates of momentum flux associated with equatorial Kelvin and gravity waves

Kaoru Sato
Department of Geophysics, Kyoto University, Kyoto, Japan

Timothy J. Dunkerton
Northwest Research Associates, Bellevue, Washington

Abstract. A new indirect method is proposed to estimate momentum flux based on the theory of slowly varying gravity waves and equatorial waves in vertical shear by *Dunkerton* [this issue] which explains the discovery by *Sato et al.* [1994] that the cospectra of temperature and zonal wind fluctuations at Singapore (1.4°N, 104.0°E) are synchronized with the quasi-biennial oscillation (QBO) of mean zonal wind in the stratosphere. The indirect estimates obtained from cospectra correspond to the summation of absolute values of momentum flux associated with each wave, whereas direct estimates from quadrature spectra give the summation of momentum flux. An analysis was made for twice daily rawinsonde data at Singapore. The direct estimate for Kelvin waves (5–20 day components) is 2–9 $\times$ 10^{-3} m^2 s^{-2} and accords with the indirect estimate to within the estimation error. This result supports the validity of the indirect method. Although the indirect estimate depends on an assumed wave structure, large values of momentum flux are obtained for all possible equatorial modes having short periods (1–3 days). The indirect estimate for westerly shear is 20–60 $\times$ 10^{-3} m^2 s^{-2} based on the theory of two-dimensional gravity waves, while the direct estimate is only 0–4 $\times$ 10^{-3} m^2 s^{-2}. The reduction of indirect estimate under the assumption of equatorial waves is about 30–70%. The discrepancy between direct and indirect estimates indicates a large cancelation of positive and negative momentum fluxes. This is the case also for easterly shear. The indirect estimate for westerly shear is almost twice as large as that for easterly shear. The characteristics of waves near the source in the troposphere are thought to be independent of the QBO in the stratosphere, so that the difference in wave activity should be attributed to the differing characteristics of wave propagation under the strong QBO shear. Several possible explanations are discussed. Parameters such as phase velocity and zonal wavelength are estimated from the ratio of potential to kinetic energies assuming that the 1–3 day components are due to equatorial waves. The estimates in this paper were made assuming that the observed frequencies are actual ground-based wave frequencies. If there is aliasing from higher frequencies than 1 day, the actual momentum fluxes can be significantly larger than the estimated values.

1. Introduction

Many theoretical and observational studies show that gravity waves play an important role in the global atmospheric circulation, redistributing momentum in the atmosphere through their generation, propagation, and breaking. The majority of studies have emphasized the role of gravity waves in the global circulation of middle- and high-latitude regions. However, we also expect energetic gravity waves associated with vigorous convection in the equatorial region. Such gravity waves may be important for the mechanism of the quasi-biennial oscillation (QBO) of mean zonal wind in the equatorial lower stratosphere as suggested by theoretical studies (see *Dunkerton* [this issue] for a review).

Observational evidence that gravity waves are important in the equatorial region, in addition to large-scale Kelvin and Rossby gravity waves, has been reported in several recent studies. *Tsuda et al.* [1994a, b] conducted a pioneering observational campaign for 24 days in Watukosek, Indonesia (7.6°S, 112.7°E), using 100 rawinsondes with vertical resolution of 150 m. Gravity waves having a vertical wavelength of 2–2.5 km and a period of about 2 days were detected in the time sequence of wind and temperature profiles. Wave propagation was eastward in the westerly shear phase of the QBO. Recently, *Takayabu et al.* [1996] examined westward propagating quasi-2-day modes in convective activity using various high-resolution data such as infrared equivalent black body temperature (T_{BB}) during the intensive observation period (IOP) of the Tropical Ocean Global Atmosphere/Coupled Ocean-Atmosphere Response Experiment (TOGA/COARE) campaign. Clear inertio-gravity wave-like signals propagating upward and downward from a ~175 hPa level were detected in composite time-height sections of horizontal winds from radiosonde observations with a reference of the quasi-2-day mode observed in T_{BB}.

The importance of gravity waves in the tropics was also shown by *Allen and Vincent* [1995], who examined gravity wave

Paper number 96JD02514.
0148-0227/97/96JD-02514$09.00

activity as a function of latitude for the range of 12°S–68°S, using rawinsonde data with high vertical resolution of 50 m, at 18 stations in Australia. The gravity wave energy increased monotonically approaching the equator, which is especially clear in summer. Such a latitudinal variation is not clear in the northern hemisphere winter as shown by *Kitamura and Hirota* [1989] using operational rawinsonde data over Japan (27°N–45°N). In their study, gravity wave energy maximized instead near the subtropical westerly jet. *Ogino et al.* [1995] examined radiosondes launched at a research vessel over a period of about 1 month during the IOP of TOGA/COARE campaign, covering a latitude range of 14°S–25°N. The energy of wave components with vertical wavelengths of 2–3 km was estimated from 112 observations in the equatorial region of 5°N–5°S and is consistent with an extrapolation of the latitudinal variation of gravity wave energy shown by Allen and Vincent.

Year-to-year variation of short-period (1–3 day) waves near the equator was examined using rawinsonde data at Singapore over the 10 years 1984–1993 by *Maruyama* [1994] and *Sato et al.* [1994] independently. Maruyama estimated momentum flux from the covariance of zonal wind and temperature tendency. He found that the momentum flux associated with short-period waves varies in a synchronized manner with the QBO and the magnitude of the flux is comparable to that of long-period (7.4–32 days) Kelvin waves. (Owing to a typographical error, the momentum fluxes are smaller than that shown in Figures 7 and 8 of *Maruyama* [1994] by exactly 1 order of magnitude (T. Maruyama, personal communication, 1996).) On the other hand, *Sato et al.* [1994] (hereinafter referred to as S94) showed year-to-year variations of spectral characteristics of horizontal wind and temperature fluctuations in the period range 1–20 days. Figure 1 shows power and cross spectra of temperature (T) and zonal wind (u) fluctuations averaged over the height region 20–25 km, in energy or flux content form, as a function of time as obtained by S94. A low-pass filter with cutoff of 6 months was applied in order to display the relation with the QBO more clearly. As mentioned in S94, dominant peaks in the power spectra of T and u are observed in the short-period range of 1–3 days during both phases of the QBO and around 10-day period in the westerly shear phase of the QBO. The latter peak corresponds to Kelvin waves, which have been examined in previous studies. Temperature spectral densities in the short-period range are large also in the easterly shear phase compared with those at longer periods, indicating that the activity of short-period waves is large in both phases of the QBO.

A mysterious feature, which was emphasized and discussed in S94, is the clear synchronization of cospectra $C_{Tu}(\omega)$ (Figure 1c) with the QBO observed in the whole range of frequencies. Positive and negative values appear alternately in the westerly and easterly shear phases, respectively, although the negative values around 10-day period are weak. Such variation was not observed in the cross spectra of meridional wind and temperature fluctuations. The variation of cospectra of T and u components cannot be explained by the previous theory of equatorial waves in a uniform background wind [*Matsuno*, 1966]. According to the theory the cospectra should be almost zero, and quadrature spectra of T and u components $Q_{Tu}(\omega)$ should have significant values proportional to $-\overline{u'w'}$ as described by *Maruyama* [1991, 1994], where w is the vertical wind component. In fact, large negative values are observed in $Q_{Tu}(\omega)$, as shown in Figure 1d, around 10 days corresponding to the positive $\overline{u'w'}$ associated with Kelvin waves, consistent with the result of *Maruyama* [1994].

Dunkerton [1995] (hereinafter referred to as D95) analyzed theoretically and numerically the covariance of horizontal wind and temperature for two-dimensional (plane) gravity waves in a background wind having vertical shear. The theory has been extended to three-dimensional equatorial waves (T.J. Dunkerton, manuscript in preparation, 1997, hereafter referred to as D97). For slowly varying, steady, conservative, incompressible waves, the covariance of zonal wind and temperature is proportional to the vertical shear and vertical flux of horizontal momentum, or radiation stress. The sign of the covariance is determined by the vertical shear, independent of the horizontal and vertical direction of gravity wave propagation, which is qualitatively consistent with the observation shown in Figure 1c.

In this paper, we examine in detail the relation between cospectra (of T and u) and the vertical shear of the mean zonal wind, using rawinsonde data at Singapore, to evaluate Dunkerton's (D95, D97) theory quantitatively (section 2). In section 3 we introduce a new method of momentum flux estimation from cross spectra (both cospectra and quadrature spectra) of T and u components, which provides positive and negative momentum fluxes separately. Such method of estimation is particularly important for short-period gravity waves which can propagate in any direction. Quantitative analysis is made for the momentum flux using Singapore data, and the results are assured by clarifying the observational error in the estimates. Further discussion is given in section 4. Summary and concluding remarks are made in section 5.

2. Comparison of Vertical Shear and Zonal Heat Flux

According to D95, the covariance of T and u components of slowly varying two-dimensional gravity waves acquires a significant value when the background wind U varies rapidly over a scale height:

For upward energy propagation

$$\overline{u'T'} = +\frac{N\bar{T}}{2gk\hat{c}}\,\overline{u'w'}U_z, \tag{1}$$

For downward energy propagation

$$\overline{u'T'} = -\frac{N\bar{T}}{2gk\hat{c}}\,\overline{u'w'}U_z, \tag{2}$$

where N is the Brunt-Väisälä frequency, g is the acceleration of gravity, k is the horizontal wavenumber which is taken to be positive without loss of generality, $\bar{T}$ is the background temperature, and $\hat{c}$ is the intrinsic phase velocity. It is convenient to express (1) and (2) with

$$\overline{u'T'} = \frac{N\bar{T}}{2gk|\hat{c}|}\,|\overline{u'w'}|U_z, \tag{3}$$

since $\overline{w'\phi'} = \hat{c}\overline{u'w'}$ and the direction of vertical energy propagation is determined by $\overline{w'\phi'}$, where ϕ' is the geopotential perturbation. It is worth noting that $\overline{u'T'}$ is proportional to U_z. The sign is determined only by the vertical shear and is independent of the direction of horizontal and vertical propagation. Thus the vertical shear of the mean wind is a key parameter to explain the covariance of u and T. The extended theory of slowly varying equatorial waves (D97) shows that the

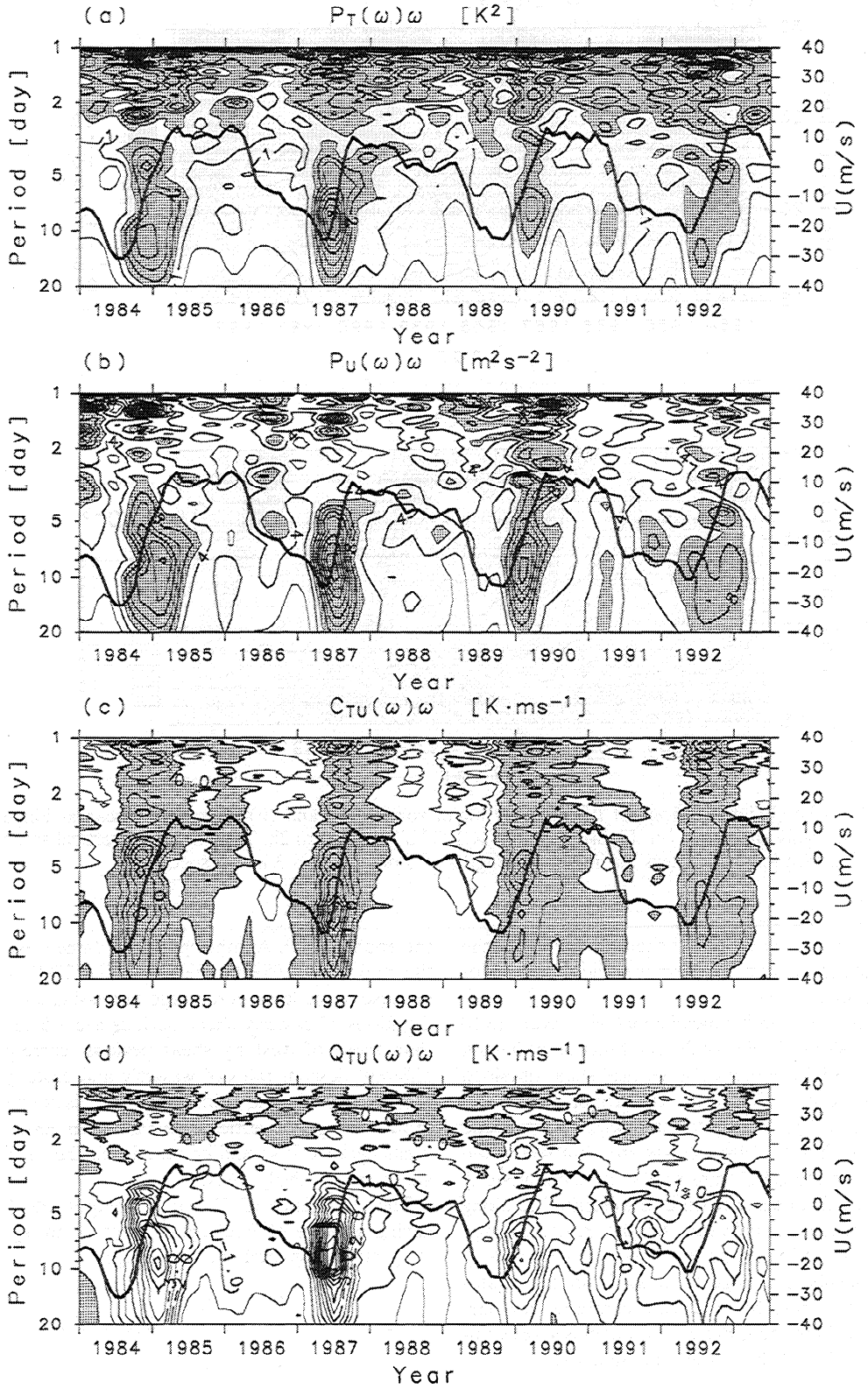

Figure 1. Dynamic power spectra of (a) temperature fluctuations T and (b) zonal wind fluctuations u in energy content form for 1984–1993, averaged over the height range 20–25 km at Singapore. (c) Cospectra and (d) quadrature spectra of T and u are also shown in flux content form. Temporal smoothing was applied using a lowpass filter with cutoff of 6 months in order to display the relation with the QBO more clearly. Thick solid curves show the monthly mean zonal wind averaged over the same height range; the scale is shown on the right axis. Contour intervals are 0.5 K^2 in Figure 1a, 2 $m^2\ s^{-2}$ in Figure 1b, and 0.5 K m s^{-1} in Figures 1c and 1d. Shading indicates values larger than 1.5 K^2 in Figure 1a, larger than 6 $m^2\ s^{-2}$ in Figure 1b, and positive values in Figures 1c and 1d.

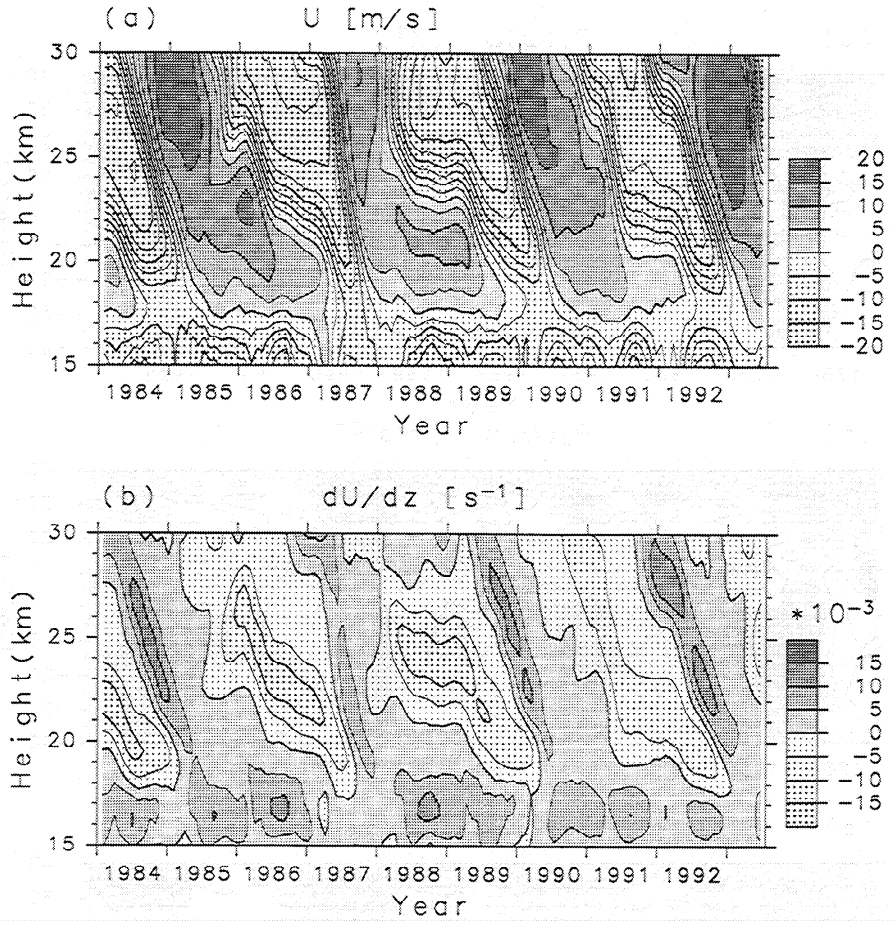

Figure 2. Time-height sections of (a) monthly mean zonal wind and (b) its vertical shear at Singapore. Contour intervals are 5 m s^{-1} in Figure 2a and 5×10^{-3} s^{-1} in Figure 2b. Temporal and vertical smoothing was applied with low-pass filters having cutoff lengths of 6 months and 3 km, respectively.

relation of the covariance and vertical shear does not change significantly except for the numerical factor in the denominator on the right-hand side of (3).

The time evolution of monthly mean zonal wind over the 10 years 1984–1993 is shown in Figure 2a as a function of height. Four cycles of the QBO are seen. The vertical shear obtained from Figure 2a is shown in Figure 2b. The tropopause is usually located around 17 km, varying annually with an amplitude of about 1 km (not shown). Large shears are observed in the lower stratosphere in the QBO transition zones from westerly wind to easterly and from easterly wind to westerly, i.e., along zero contours of the mean zonal wind. Another region of large vertical shear is observed near the tropopause where easterly winds in the troposphere change to westerly in the stratosphere. The easterly phase below 20 km continues for only one-fourth or one-fifth of the QBO cycles, which is short compared with the duration of the easterly phase above.

Subsequent sections are devoted mainly to the lower stratosphere above 20 km where the QBO is clearly seen in the vertical shear. We define three periods of large westerly (positive) shear as A (from the beginning of 1984 to the middle of 1985), B (from the beginning to the end of 1987), and C (from the beginning of 1992 to the beginning of 1993); and three periods of large easterly (negative) shear as a (from the beginning of 1986 to the middle of 1987), b (from the beginning of 1988 to the beginning of 1990), and c (from the end of 1990 to the end of 1992). Another period of large westerly shear from the middle of 1989 to the middle of 1990 is not examined because of the large percentage of missing data (see S94). The durations of easterly shear periods are 1.5 to 2 times longer than those of westerly shear periods, corresponding to the different descent rates of westerly and easterly phases of the QBO. An interesting point is that there is not a large difference in the strength of vertical shear between easterly and westerly shear periods. It should be noted that the shears in periods B and c are relatively weak.

The covariance of T and u components ($C_{Tu} \equiv \overline{T'u'}$) having a range of frequencies from ω_1 to ω_2 is obtained by integrating cospectra over the range

$$C_{Tu} \equiv \int_{\omega_1}^{\omega_2} C_{Tu}(\omega)\, d\omega, \tag{4}$$

where ω is ground-based frequency. Similarly, we can define Q_{Tu} as an integration of quadrature spectra over the same frequencies:

$$Q_{Tu} \equiv \int_{\omega_1}^{\omega_2} Q_{Tu}(\omega)\, d\omega \approx \frac{1}{|\omega_0|} \overline{\frac{\partial T'}{\partial t}}\, u', \tag{5}$$

where ω_0 is the central (ground-based) frequency of the inte-

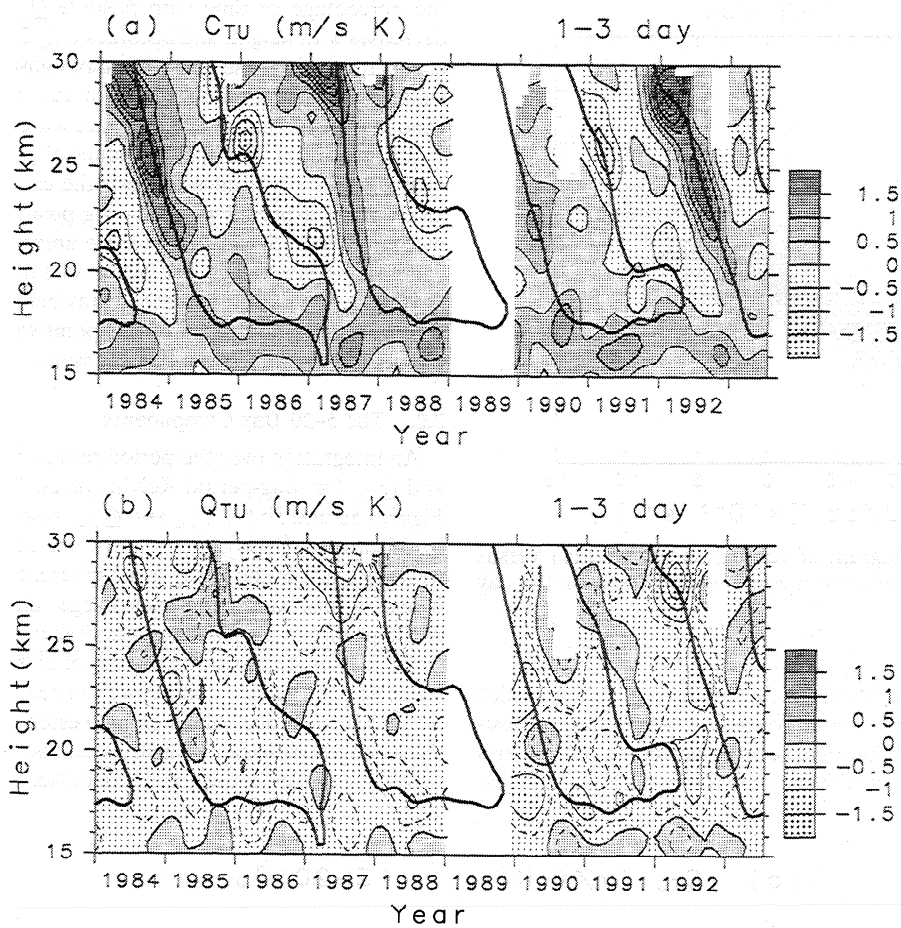

Figure 3. Time height sections of (a) cospectra of temperature and zonal wind components C_{Tu} and (b) that of quadrature spectra Q_{Tu} integrated over the period range of 1–3 days. Thick curves indicate zero contours of the monthly mean zonal wind shown in Figure 2. Contour intervals are 0.5 K m s^{-1}. Dashed curves in Figure 3b are the contours of 0.25 and −0.25 K m s^{-1}. Filters used for smoothing are the same as those for Figure 2.

gration range. From the thermodynamic equation, Q_{Tu} is related to total momentum flux:

$$Q_{Tu} \sim -\mathrm{sgn}(\omega_0)\,\frac{\bar{T}N^2}{g\hat{\omega}}\,\overline{u'w'}, \qquad (6)$$

where $\hat{\omega}$ is the intrinsic frequency of waves having the central frequency ω_0.

2.1. The 1–3 Day Components

Figure 3a shows a time-height section of C_{Tu} for 1–3 day wave components, which are considered to be due mainly to gravity waves. Blank regions indicate where an estimate could not be made due to a large number of missing values. Large positive and negative values are observed along westerly and easterly shear zones, respectively, which is qualitatively consistent with the theory of D95. It is interesting that there seems to be a good quantitative correspondence as well, although the magnitude of C_{Tu} should depend on $\overline{u'w'}$ as well as U_z. Large (small) values are observed in strong (weak) shear at periods A, C, a and b (B and c).

To see the details of the correlation, a scatter diagram was made (Figure 4) using data from the cross sections of C_{Tu} and the vertical shear of mean zonal wind. Clear linear distribution is seen in regions of positive and negative vertical shear. The number of events having positive (negative) C_{Tu} in negative (positive) shear is small, especially when the shear is strong. This fact supports the theory of D95.

The gradient of the linear distribution in positive shear seems larger than that in negative shear. Thin straight lines are the result of a least squares fit in the respective regions. The slopes of the lines differ by a factor of about 2.5. If we ignore the Doppler shift of wave frequency by the mean wind, the slope is proportional to momentum fluxes according to (3). Thus the difference suggests that the momentum flux of 1–3 day waves is larger in westerly shear than in easterly shear. The difference in momentum fluxes between westerly and easterly shear periods will be quantitatively discussed in section 4.3 showing their vertical profiles.

The time-height section of Q_{Tu} for 1–3 day components is shown in Figure 3b. It is obvious that Q_{Tu} values are small compared with C_{Tu} (Figure 3a). However, since the variation of Q_{Tu} observed in Figure 3 is slightly larger than the error in Q_{Tu} (and C_{Tu} also) which is about 0.2 m s^{-1} K as estimated later, some qualitative discussion of Q_{Tu} is possible.

The Q_{Tu} observed in Figure 3 is biased toward negative values over the whole region, indicating the relative dominance of eastward propagating waves, and is consistent with the results of *Maruyama* [1994]. The bias may be due to selective

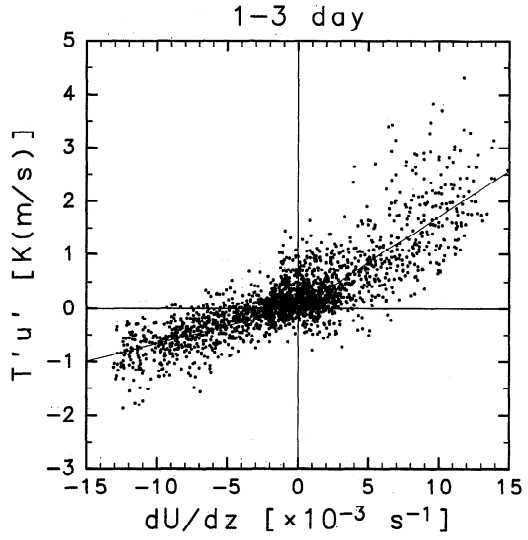

Figure 4. Scatter diagram of vertical shear (dU/dz) versus covariance of temperature and zonal wind ($T'u'$) of 1–3 day components.

transmission in easterly winds of the upper troposphere, which inhibit the vertical propagation of gravity waves having westward phase speed. If the wave sources are below 15 km, this speculation is consistent with the observation in Figure 3b that the percentage of time with positive Q_{Tu} is 45% at 15 km, decreases with height, and becomes only 2% at 18 km. Another explanation is that the distribution of phase velocities of gravity waves generated by convection in the easterly tropospheric wind may be biased toward eastward waves [*Pfister et al.*, 1993].

It is important that positive values of Q_{Tu} are seen in places of Figure 3. This feature suggests the existence of at least two kinds of short-period waves having positive and negative momentum fluxes. Systematic positive areas above easterly shear zones may be explained also by the shielding of eastward propagating waves due to westerly winds below the shear zone. A comprehensive discussion of this point will be made based on the results of momentum flux estimation in section 3.

2.2. The 5–20 Day Components

An integration over the period range of 5–20 days gives C_{Tu} and Q_{Tu} for long-period Kelvin waves. Results are shown in Figures 5a and 5b for C_{Tu} and Q_{Tu}, respectively. As reported by *Maruyama* [1994], Q_{Tu} values are largely negative along westerly shear in the lower stratosphere, corresponding to positive $\overline{u'w'}$ due to Kelvin waves. Large values are also observed in the profile of C_{Tu} along westerly shear. The sign is positive, which is consistent with the theory of D95. On the other hand, negative C_{Tu} values along easterly shear are very weak compared with positive values along westerly shear, even though the strength of easterly shear is almost the same as that of westerly shear, as already mentioned. According to the theory of

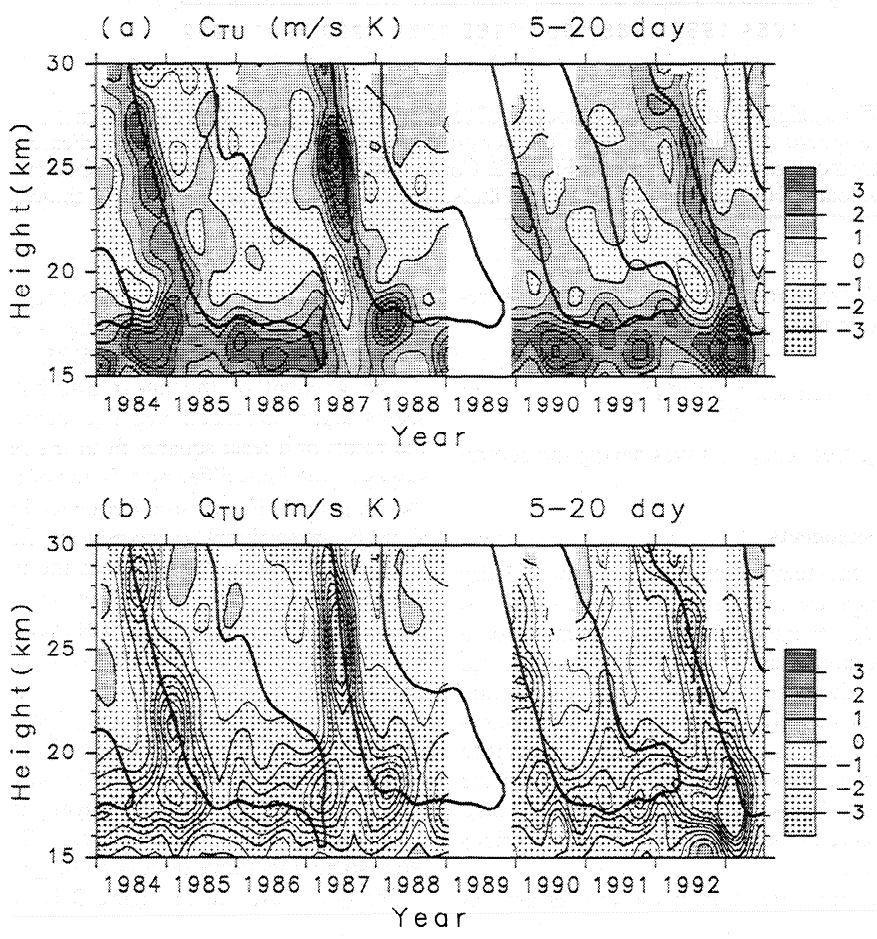

Figure 5. Integrated cospectra and quadrature spectra as in Figure 3 but for the period range 5–20 days. Contour interval is 1 K m s^{-1}.

D95, small values of cospectra mean that amplitudes of individual wave components in the period range of 5–20 days are very small.

Also interesting is the feature near the tropopause where large positive values of C_{Tu} and negative values of Q_{Tu} are continuously observed. *Tsuda et al.* [1994a] reported slow Kelvin waves which are dominant around the tropopause and modulate the tropopause height. Figure 5 suggests that such Kelvin waves are common. It is likely that the dominance of Kelvin waves is related to the long duration of westerly wind above the tropopause (around 20 km).

Figure 6 shows a scatter diagram for 5–20 day components in the 20–30 km height region. The values of C_{Tu} in positive shear are mostly positive and linearly proportional to the shear. The correlation, however, is not high compared with that of 1–3 day components (Figure 4), indicating that the variation of Kelvin wave activity is larger. A bias of C_{Tu} toward negative values in negative shear is unclear. Solid straight lines show the result of a least squares fit. The ratio of slopes for positive versus negative shear is larger than 7. Thus it is suggested that long-period wave activity in easterly shear is less than in westerly shear by about 1 order of magnitude.

It was found from the analysis in this section that most features of C_{Tu} are consistent with the theory of gravity or equatorial waves in vertical shear [D95, D97], and it was suggested that C_{Tu} includes important information on the wave characteristics. Therefore, we use this theory to estimate momentum flux quantitatively in section 3.

3. Estimates of $\overline{u'w'}$ Based on Cross Spectra of T and u

3.1. Methods of Direct and Indirect Estimation

Using (3) and (6), we can make two kinds of estimates of momentum flux under the assumption of two-dimensional gravity waves.

The first is a direct method from quadrature spectra of T and u fluctuations:

$$\overline{u'w'} = -\frac{g}{\bar{T}N^2}\int_{\omega_1}^{\omega_2} Q_{Tu}(\omega)\,\omega\,d\omega, \tag{7}$$

where ω_1 and ω_2 are lower and upper limits of the frequency range that we are interested in. The Doppler effect of mean wind is ignored, since the mean wind around the large shear is weak. We use 220K for $\bar{T}$ and 5 min for the Brunt-Väisälä period as typical values in the lower stratosphere. The direct estimate of $\overline{u'w'}$ is composed of positive $(\overline{u'w'})_+$ and negative $(\overline{u'w'})_-$ momentum fluxes:

$$\overline{u'w'} = (\overline{u'w'})_+ + (\overline{u'w'})_-. \tag{8}$$

Observations suggest that the short-period waves propagate energy predominantly upward in the equatorial lower stratosphere [e.g., *Tsuda et al.*, 1994; *Maruyama*, 1994; S94]. Thus, if we assume that the waves are mainly propagating upward, $(\overline{u'w'})_+$ and $(\overline{u'w'})_-$ are due to eastward and westward propagating waves, respectively. It is also possible that the cancelation is partly due to reflected waves propagating downward [D95].

The second is an indirect method from cospectra of T and u fluctuations:

$$|\overline{u'w'}| = \frac{2g}{N\bar{T}U_z}\int_{\omega_1}^{\omega_2} C_{Tu}(\omega)\,\omega\,d\omega, \tag{9}$$

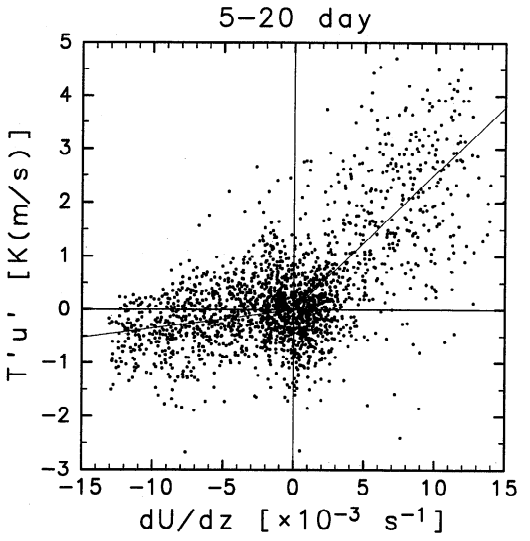

Figure 6. As in Figure 4, but for 5–20 day components.

under the assumption that the disturbances are due to two-dimensional gravity waves. The factor on the right hand side of (9) must be modified for equatorial waves as noted in section 2. The indirect estimate of $|\overline{u'w'}|$ is the sum of absolute values of $\overline{u'w'}$ of all waves having a frequency in the particular range which we considered:

$$|\overline{u'w'}| = |(\overline{u'w'})_+| + |(\overline{u'w'})_-|. \tag{10}$$

Therefore, using (8) and (10), we can obtain $(\overline{u'w'})_+$ and $(\overline{u'w'})_-$ separately.

It should be noted that the indirect estimate of momentum flux from C_{Tu} is possible only when the wind shear is large and when the mean wind is sufficiently weak not to cause severe Doppler effect. For this paper, we made direct and indirect estimates when the strength of wind shear $|U_z|$ is larger than 5×10^{-3} s^{-1} and that of mean zonal wind $|U|$ is smaller than 5 m s^{-1} for the positive shear periods (A, B, and C) and negative shear periods (a, b, and c). Four frequency bands were examined, corresponding to 1–3 day, 3–5 day, 5–20 day, and 1–20 day periods.

Ignoring the Doppler effect by the mean wind may cause uncertainty for the momentum flux estimate, but it is probably not severe. For example, the most severe error caused by the mean wind of 5 m s^{-1} for waves with a period of 1.5 day and a zonal wavelength of 3000 km, which is a typical value as shown later, is only a few tens percent, so that the uncertainty in the value averaged over each shear period would be negligible. The validity of the assumption of two-dimensional gravity waves is discussed later.

3.2. Accuracy of Momentum Flux Estimates

Before discussing the estimates of momentum flux, the observational error is considered. Here we use the notation of error(A) as the error in a physical quantity A.

The observational error of temperature and winds depends on the method and performance of the device used for rawinsonde observations at Singapore and is not easy to evaluate. However, we can estimate the error roughly from the observational data. As mentioned in S94, clear wave-like structures observed in a time-height section of high-pass filtered T and u components have amplitudes of about 1 K and 2 m s^{-1}, re-

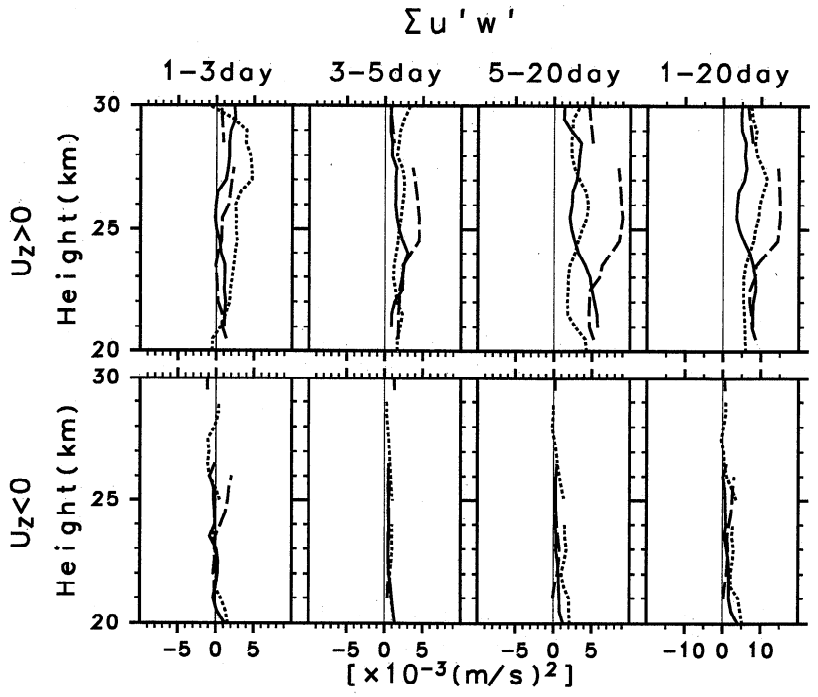

Figure 7. Direct estimate of momentum flux $\overline{u'w'}$ as a function of height for period ranges of 1–3 days, 3–5 days, 5–20 days, and 1–20 days, during time periods when the vertical shear is (top) greater than 5×10^{-3} s^{-1} and (bottom) less than -5×10^{-3} s^{-1}. Solid, long-dashed, and short-dashed curves in the top (bottom) figures are estimates in time periods A (a), B (b), and C (c), respectively.

spectively. The error in the original data is considered to be almost the same as that of the high-pass filtered profiles and is safely assumed to be no more than 0.5 K for error[T] and 1 m s^{-1} for error[u] (i.e., one-half of the wave amplitude).

Further, it is safely assumed that the observational errors in T and u are independent of time, and there is no correlation between the errors. Since the frequency spectrum of such errors is white, the error in Q_{Tu} (and C_{Tu}) is

$$\text{error}[Q_{Tu}] = \text{error}[C_{Tu}] = \sigma_T \frac{\text{error}[u]}{\sqrt{n_s}} + \sigma_u \frac{\text{error}[T]}{\sqrt{n_s}} + \frac{\text{error}[u]\text{error}[T]}{n_s}, \tag{11}$$

where σ_T and σ_u are square roots of the variance of T and u fluctuations having frequencies in the integrated range, respectively, and n_s is the number of integrated spectral points. The last term on the right-hand side of (11) can be ignored when n_s is sufficiently large.

For 1–3 day (5–20 day) components, σ_T and σ_u are about 1.5 K (2 K) and 2.5 m s^{-1} (5 m s^{-1}), respectively, and n_s is 120 (28) for the spectra calculated using a window of 3 months. Since the average in each of the large shear periods was made for at least 6 months, n_s should be doubled, i.e., 240 for 1–3 day components and 56 for 5–20 day components. Using these values, we obtain error[Q_{Tu}] and error[C_{Tu}] of 0.2 K m s^{-1} for 1–3 day components and 0.6 K m s^{-1} for 5–20 day components.

The observational errors in momentum flux obtained by the direct and indirect methods are estimated from the values of error[Q_{Tu}] and error[C_{Tu}]:

$$\text{error}[\overline{u'w'}] \sim \frac{g\omega_0}{\bar{T}N^2}\,\text{error}[Q_{Tu}], \tag{12}$$

$$\text{error}[|\overline{u'w'}|] \sim \frac{2g\omega_0}{N\bar{T}U_z}\,\text{error}[C_{Tu}], \tag{13}$$

where ω_0 is the central frequency of the integration range. As a result, we obtained almost the same values of error for 1–3 day and 5–20 day components:

$$\text{error}[\overline{u'w'}] = 5\text{–}8 \times 10^{-4}\ \text{m}^2\,\text{s}^{-2}, \tag{14}$$

for direct estimates, and

$$\text{error}[|\overline{u'w'}|] = 4\text{–}8 \times 10^{-3}\ \text{m}^2\,\text{s}^{-2} \quad |U_z| = 5 \times 10^{-3}\ \text{s}^{-1}, \tag{15}$$

$$\text{error}[|\overline{u'w'}|] = 2\text{–}4 \times 10^{-3}\ \text{m}^2\,\text{s}^{-2} \quad |U_z| = 10 \times 10^{-3}\ \text{s}^{-1}, \tag{16}$$

for indirect estimates. It should be noted again that the estimated errors are the largest (i.e., most pessimistic) estimates and hence the real accuracy must be better than this at lower levels where missing data are few. At upper levels, however, the error may be larger because the percentage of missing data becomes larger [S94]. The error of indirect estimates assuming equatorial waves is modified corresponding to the modification for (9).

3.3. Results of Direct Estimation

Direct estimates of $\overline{u'w'}$ were obtained from quadrature spectra using (7). Profiles of momentum flux were averaged

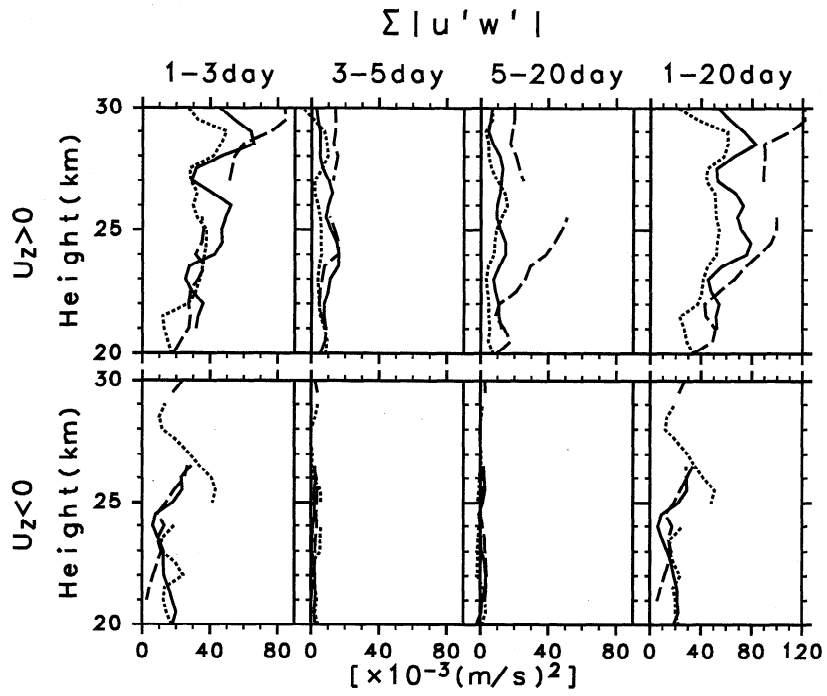

Figure 8. As in Figure 7, but for the indirect estimate of momentum flux $|\overline{u'w'}|$.

over each of positive shear periods (A, B, and C) and negative shear periods (a, b, and c). The mean values of $\overline{u'w'}$ are plotted separately for 1–3 day, 3–5 day, 5–20 day, and 1–20 day components in Figure 7 as a function of height. Different line styles show different time periods. The reader is cautioned that the vertical profiles of $\overline{u'w'}$ were obtained for periods of large shear, and the time of observation depends on altitude (see Figure 2). Therefore the displayed vertical profiles of momentum flux do not provide the wave drag from its convergence.

For westerly shear ($U_z > 0$), values of $\overline{u'w'}$ are biased toward positive in all frequency ranges. The momentum flux associated with 1–3 day components is about $0–5 \times 10^{-3}$ m^2 s^{-2}, and tends to increase with height from 1×10^{-3} m^2 s^{-2} at 22 km to 3×10^{-3} m^2 s^{-2} at 28 km, on average. The estimate is meaningful because the average values are larger than the error estimated in the previous section.

The momentum flux for long-period (5–20 day) Kelvin waves in westerly shear is $2–9 \times 10^{-3}$ m^2 s^{-2}. These values are a little smaller than the estimate from previous observational studies of $\sim 6 \times 10^{-3}$ m^2 s^{-2} [e.g., *Andrews et al.*, 1987]. It should be noted, however, that the quadrature spectra due to Kelvin waves in Figure 1 is spread over a wide range of periods extending from about 20 days to 3 days. It may be better to examine the sum of 3–5 day and 5–20 day components, which is $4–12 \times 10^{-3}$ m^2 s^{-2} and comparable to previous studies.

The total momentum flux in westerly shear associated with 1–20 day components is about $4–15 \times 10^{-3}$ m^2 s^{-2}. The contribution by long-period Kelvin waves is largest, and the momentum flux due to 1–3 day components is about half as large.

On the other hand, the momentum flux in easterly shear is generally small compared with that in westerly shear. For 5–20 day components, positive bias due to Kelvin waves around the tropopause is observed at lower levels and the momentum flux is comparable to the error above 26 km. The momentum flux associated with 1–3 day components is weakly negative above 26 km, corresponding to systematic positive values of Q_{Tu} around easterly shear observed in Figure 3, although the momentum flux below is distributed around zero. The total momentum flux in easterly shear for 1–20 day components is about $2–6 \times 10^{-3}$ m^2 s^{-2} at lower levels, decreasing with height and almost zero at upper levels.

3.4. Results of Indirect Estimation

The results from indirect estimation of momentum flux using (9) are summarized in Figure 8 in the same manner as the direct estimate (Figure 7). The indirect estimates should accord with those of the direct estimation if momentum fluxes associated with waves in the period range are of one sign.

First, let us examine the results for 5–20 day components in westerly shear, in which we expect dominance of long-period Kelvin waves. The vertical profiles of indirect estimates in Figure 7 are similar to those of direct estimates, although the indirect estimates of momentum flux ($3–50 \times 10^{-3}$ m^2 s^{-2}) are larger than the direct estimates ($2–9 \times 10^{-3}$ m^2 s^{-2}).

According to the extended theory for equatorial waves [D97], the factor in (9) is ⅔ instead of 2 if the disturbances are due to Kelvin waves. Thus the indirect estimate for 5–20 day components is likely to be overestimated by a factor of 3/2. This modification makes the indirect estimates almost consistent with results from the direct method, except for period B (long-dashed curves) which has significantly larger values compared with the other two periods A and C. The large amplitudes for period B suggest that nonlinear effects such as "saturation" are not negligible [D95]. In such cases, the covariance of T and u components can be larger than expected from (3). Figure 9 shows the modified profiles of indirect estimates for periods A and C (thin curves). Direct estimates for the same time periods are plotted by thick curves for comparison. The difference between modified indirect estimates and direct estimates for A and C profiles is $0–4 \times 10^{-3}$ m^2 s^{-2}, which is within the estimation error of the indirect method. The consistency between the results of direct and indirect estimation

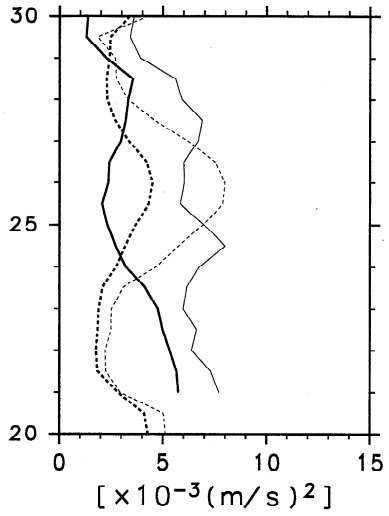

Figure 9. Vertical profiles of indirect estimates of momentum flux for 5–20 day components in time periods A (solid) and C (dashed) based on the theory of equatorial Kelvin waves (thin curves). The direct estimates of momentum flux for the same time periods and wave components are shown by thick curves for comparison.

for long-period Kelvin waves supports the validity of the indirect method.

The most important feature in Figure 8 is that the indirect estimates of the momentum flux associated with short-period (1–3 day) components are significantly large and occupy the largest portion of the total (1–20 day) momentum flux in both westerly and easterly shears. The magnitude of indirect estimates of momentum flux due to 1–3 day components in westerly shear is about 20×10^{-3} m^2 s^{-2} at 21 km, increases with height, and becomes 50×10^{-3} m^2 s^{-2} at 30 km, which is almost 10 times larger than the direct estimates of $0–5 \times 10^{-3}$ m^2 s^{-2}. This fact indicates that 1–3 day components are composed of at least two kinds of waves having positive and negative momentum fluxes and that large momentum fluxes associated with the waves are cancelled in the sum. Assuming that short-period waves propagate mainly upward, the momentum flux of waves in one direction (eastward or westward) must be almost one-half of the indirect estimate, and significantly larger than the momentum flux due to long-period Kelvin waves. The difference between the three periods of A, B, and C is small, reflecting the high correlation of C_{Tu} and vertical shear observed in Figure 4.

In easterly shear, the 1–3 day components are dominant again. The momentum fluxes are $7–30 \times 10^{-3}$ m^2 s^{-2} which are nearly half of those in westerly shears. The difference in momentum fluxes affects largely the difference in the gradient of the distribution between westerly and easterly shear periods in the scatter diagram of Figure 4. The indirect estimates are much larger than the direct estimates which are smaller than 3×10^{-3} m^2 s^{-2}, suggesting that the large cancelation between positive and negative momentum fluxes occurs also in easterly shear. This is consistent with the Q_{Tu} profile, in which the sign changes around the large shear as discussed in section 2.1. On the other hand, indirect estimates for 3–5 and 5–20 day components are small, consistent with the direct estimates. This fact means that the amplitudes of individual longer-period waves in easterly shear is small at the equator.

3.5. Possibility of Equatorially Trapped Waves for 1–3 Day Components

In section 3.4 we assumed that 1–3 day components are due to two-dimensional gravity waves. This assumption may be valid near source regions, i.e., at lower levels in the stratosphere, where the horizontal (in particular, the meridional) expanse of wave packets is too small to feel the beta effect of the earth rotation. It is likely, however, that as the waves propagate upward, their localized structure disappears and the waves acquire the structure of equatorially trapped modes. Thus, in this section we consider the possibility of equatorial waves for 1–3 day components and examine the modification of indirect momentum flux estimate.

An important quantity to examine the structure of equatorially trapped waves is the ratio of potential energy (PE) and kinetic energy (KE), which depends on the mode index n characterizing the meridional structure, the nondimensional zonal wavenumber $k^*(\equiv ky_0)$, and the nondimensional wave frequency $\omega^*(\equiv \omega/\beta y_0)$, where y_0 $(\equiv \sqrt{N/|m|\beta})$ is the latitudinal scale factor and β is 2.283×10^{-11} m^{-1} s^{-1} at the equator. Figure 10a shows the dispersion curves for odd IGW modes ($n = 1, 3, 5, \cdots$) and Kelvin modes ($n = -1$) which have a nonzero u component at the equator (i.e., at Singapore). The dispersion relation is

$$\omega^{*2} - \frac{k^*}{\omega^*} - k^{*2} = 2n + 1 \tag{17}$$

The upper limit of $\omega^* \sim 4$ in Figure 10a corresponds to a minimum vertical wavelength of 2 km for the central frequency $(1.5 \text{ days})^{-1}$ in the period range of 1–3 days, which is detectable by routine rawinsonde observations in the lower stratosphere with vertical resolution of about 1 km. At the equator, assuming that latitudinal shear is $O(y)$, the ratio (R) of PE to zonal KE (i.e., the contribution to KE by u component) is

$$R \equiv \frac{\text{PE}}{\text{zonal KE}} = \frac{\phi'^2/N^2}{\phi'^2/c^2} \sim \frac{m^2\omega^2}{N^2k^2} = \frac{\omega^{*2}}{k^{*2}}, \tag{18}$$

where m is vertical wavenumber. Figure 10b shows R, which is 1 for Kelvin waves and larger than 1 for IGWs. It should also be noted that for two-dimensional hydrostatic gravity waves,

$$\text{PE/KE} \sim 1. \tag{19}$$

Figure 10c shows the correction factor C which is used to obtain an indirect estimate of momentum flux for equatorial waves $\overline{|u'w'|}_{\text{eq}}$ from our earlier estimate under the assumption of two-dimensional gravity waves $\overline{|u'w'|}_{\text{2-dim}}$:

$$\overline{|u'w'|}_{\text{eq}} = C\overline{|u'w'|}_{\text{2-dim}}, \tag{20}$$

where

$$C \equiv \frac{1}{2}\left[\left(1 - \frac{k^{*2}}{4|\omega^*|W_g^*}\right)\frac{\omega^*}{k^*}\right]^{-1} \tag{21}$$

and

$$W_g^* \equiv \frac{\omega^*(\omega^{*2} + k^{*2} + k^*/\omega^*)}{2\omega^{*2} + k^*/\omega^*}. \tag{22}$$

is the nondimensional vertical group velocity [D97]. The correction factor C is smaller than 1 for all equatorial Kelvin and inertia-gravity waves. For the equatorial inertia-gravity waves, the correction factor C decreases as R increases for one mode.

Thus the momentum flux obtained under the assumption of two-dimensional gravity waves in the previous section may be overestimated. However, it is shown in the following that the modification is too small to affect our conclusion that there is a large cancelation of positive and negative momentum fluxes for 1–3 day components.

Figures 11 and 12 show the zonal KE ($\overline{u'^2}$) and PE ($\overline{(T'g/\bar{T}N)^2}$), respectively (divided by density), in the same manner as Figures 7 and 8. The contribution of meridional wind component to KE ($\overline{v'^2}$; meridional KE divided by density) is shown in Figure 13.

In westerly shear ($\bar{U}_z > 0$), PE is larger than zonal KE for 1–3 day components below 25 km, which is consistent with the characteristics of equatorial inertia-gravity waves with odd n. It should be noted that meridional KE is as large as zonal KE in this height region and that total KE (zonal KE plus meridional KE) is comparable to PE. It is possible that the meridional KE is due to Rossby gravity waves or other modes with even n. However, if we take into account that the height region is near the source of the waves, there is another possibility that the zonal KE and meridional KE belong to the same disturbances whose wave vector has both zonal and meridional components. In fact, wave-like structure is sometimes observed in the meridional wind component in the lower stratosphere below 25 km (see Figure 4b of S94). The equipartition of PE and total KE in this height region is consistent with the assumption of two-dimensional gravity waves used in the momentum flux estimation in section 3.4.

Such waves having a meridional component of the wave vector would propagate outward from the equator, refract back and forth in the equatorial waveguide [e.g., *Gill*, 1982] while propagating upward, so that zonally oriented equatorial modes would form in the upper region. This scenario is consistent with the fact that zonal KE is larger than meridional KE above 25 km. It is important that the zonal KE is almost equal to PE for 1–3 day components above 25 km. This is again consistent with the assumption of zonally oriented plane gravity waves used for momentum flux estimation in the previous section. However, it is also the case for equatorial Kelvin waves (see Figure 10b).

Let us consider the hypothesis that the 1–3 day waves are composed only of equatorial Kelvin waves. In this case, the momentum flux obtained from two-dimensional gravity wave theory is overestimated by a factor of ½ as for long-period Kelvin waves. Using the value of 50×10^{-3} m^2 s^{-2} above 25 km in Figure 8, we obtain a (modified) indirect estimate of 33×10^{-3} m^2 s^{-2}. However, this value is still much larger than the direct estimate of $\sim 2 \times 10^{-3}$ m^2 s^{-2} shown in Figure 7 which is independent of wave characteristics. Thus the indirect estimate cannot be explained by Kelvin waves alone, and we need to consider the coexistence of other kinds of waves.

It is worth noting that radiative damping can modify the ratio of PE and KE of waves. According to equatorial wave theory, Kelvin waves should have equal PE and zonal KE. This is the case for long-period Kelvin waves below 24 km (see Figures 12 and 11). However, KE is larger than PE above 24 km. The reduced PE is likely due to radiative damping. The maximum reduction seems about 50%. Such damping may occur also for 1–3 day components but is probably smaller.

Let us consider another hypothesis that the 1–3 day waves are composed of an equatorial wave having R of 2, assuming 50% reduction of PE by radiative damping so as to obtain the minimum, i.e., most severe correction factor C. Possible modes

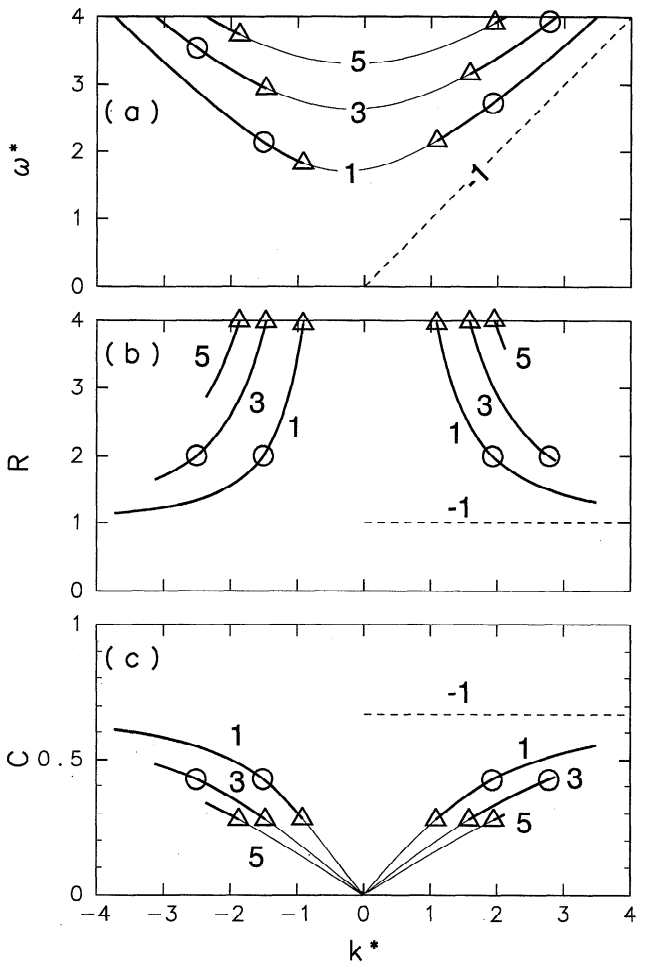

Figure 10. (a) Dispersion curves of odd modes of equatorial inertia-gravity waves (solid curves) and Kelvin wave (dashed line). Horizontal and vertical axes show nondimensional zonal wavenumber and frequency. (b) The ratio of potential energy to kinetic energy (R). (c) Correction factor (C) to obtain indirect estimates of momentum flux from the estimate based on two-dimensional gravity wave theory. Open circles and triangles are modes having R of 2 and 4, respectively. Thick curves show the inertio-gravity modes with R smaller than 4 for observed 1–3 day components.

are denoted by open circles, and the correction factor C is about 0.42. Thus the indirect estimate of momentum flux above 25 km is about 20×10^{-3} m^2 s^{-2} which is still much larger than the direct estimate of $\sim 2 \times 10^{-3}$ m^2 s^{-2}.

In easterly shear, zonal KE is relatively large for the period range of 5–20 days and 1–3 days. The zonal KE for 5–20 days is slightly larger than PE as seen in westerly shear. Judging by the dominance of zonal KE at long periods, the 5–20 day components are likely due to Kelvin waves which leak through the westerly wind below. The 1–3 day components have PE about twice as large as zonal KE, independent of height. Considering the most severe reduction (50%) by radiative damping again, we can assume that 1–3 day components are due to inertia-gravity waves at upper levels, R of which is 4. The corresponding correction factor C is 0.28 (denoted by triangles in Figure 10). The momentum flux modified under the assumption of equatorial inertia-gravity waves is then $2–8 \times 10^{-3}$ m^2

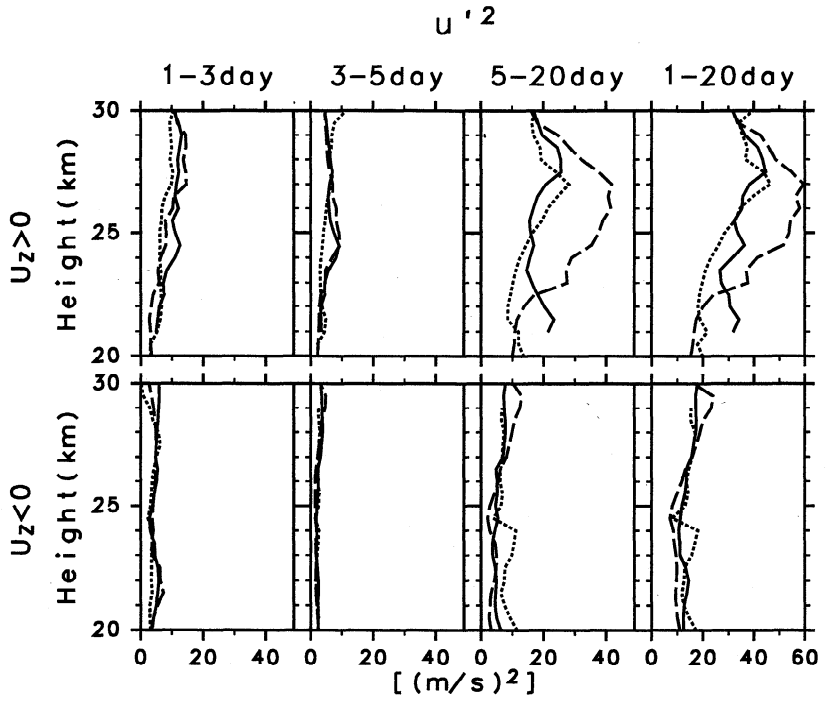

Figure 11. As in Figure 7, but for the kinetic energy (divided by density) due to zonal wind component.

s^{-2}, which is still considerably larger than the direct estimate (note that the direct estimate is small compared to the error). It is also worth noting that meridional KE is large even at upper levels, in particular for 1–3 and 3–5 day components. This feature corresponds to the dominance of Rossby gravity waves along easterly shear zones shown by S94.

From the discussion above, it is concluded that we cannot explain the difference between direct and indirect estimates of momentum flux for 1–3 day components in both easterly and westerly shears without taking into consideration the coexistence of multiple waves having positive and negative momentum fluxes. This conclusion is also supported by Q_{Tu} showing a complicated distribution of positive and negative values in the time-height section of Figure 3.

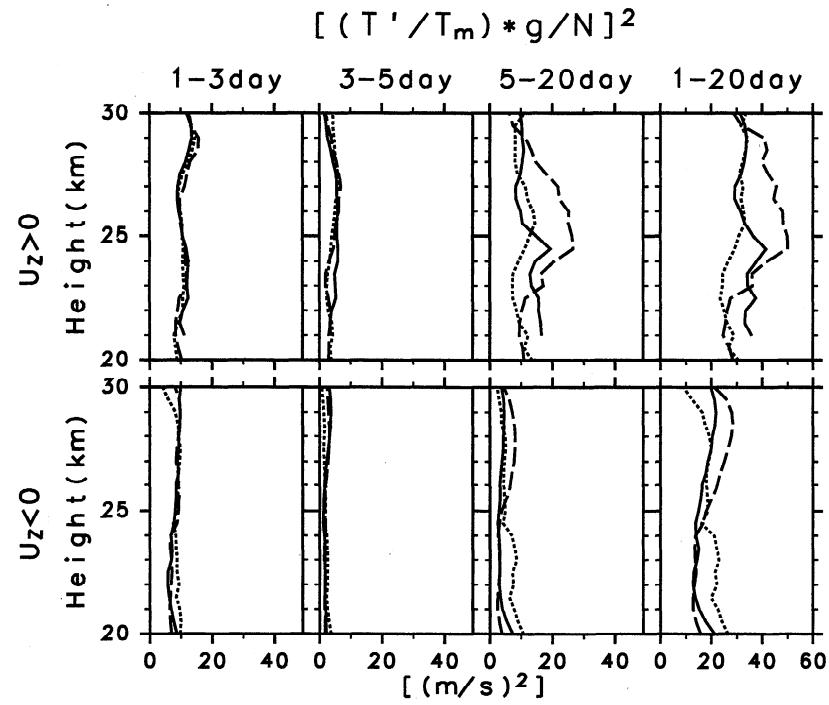

Figure 12. As in Figure 7, but for the potential energy (divided by density).

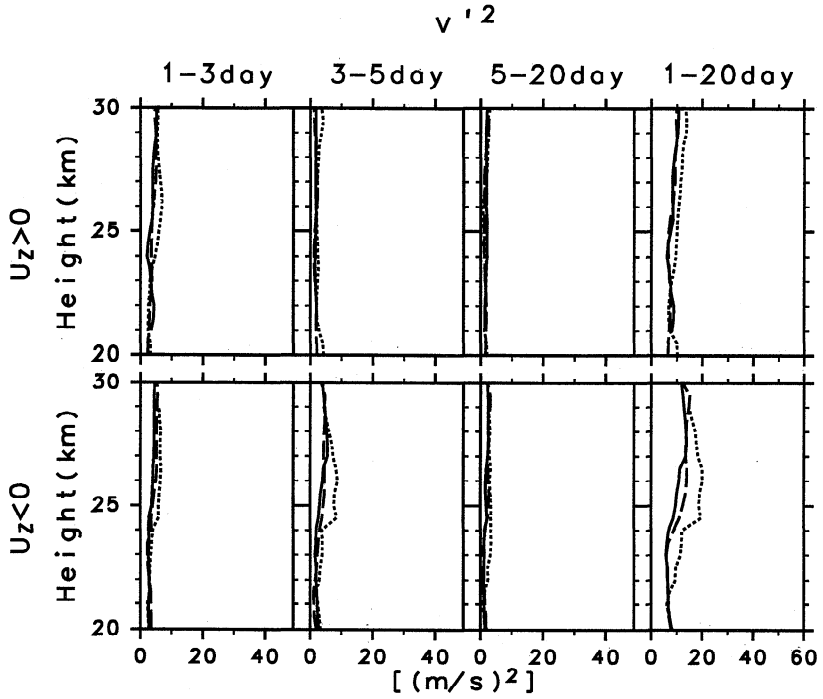

Figure 13. As in Figure 7, but the kinetic energy (divided by density) due to meridional wind component.

4. Discussion

4.1. Difference Between Easterly and Westerly Shears

It was shown in the previous section that there are some differences in wave characteristics for 1–3 day components between easterly and westerly shears. The indirect estimate of momentum flux was larger in westerly shear than in easterly shear. The ratio of potential energy to kinetic energy is smaller in westerly shear than in easterly shear. If wave spectra in the source region (i.e., troposphere) are independent of the QBO in the lower stratosphere, the differences that depend on the QBO must be attributed to propagation in the lower stratosphere below QBO shear zones, assuming that the waves are mainly propagating energy upward. Several possible explanations are listed below.

First, there may be asymmetry in the phase velocity spectra of short-period waves emerging from the troposphere. Since the easterly (westerly) wind below the westerly (easterly) shear inhibits upward propagation of westward (eastward) waves, the dominance of wave activity in westerly shear may be due to dominance of eastward waves in the source spectra. This is likely because the mean wind in the upper troposphere is easterly in convective regions such as the Maritime Continent (see Figure 2). The "topographic" effect of convection in an easterly mean wind will generate a phase velocity spectrum biased toward eastward waves [e.g., *Pfister et al.*, 1993]. Even if eastward and westward gravity waves are generated equally at some lower levels in the troposphere, gravity waves with westward phase velocities comparable to the easterly wind in the upper troposphere cannot propagate to the tropopause.

Second, differences may be due to an asymmetric manifold of equatorial waves, i.e., the asymmetry of dispersion curves around $k^* = 0$ (see Figure 10). If 1–3 day components are due mainly to equatorial waves, the characteristics of propagation can be asymmetric even if the QBO of mean zonal wind is symmetric. An extreme case is that of Kelvin waves below $\omega^* \approx 2$ (for 5–20 day components): there is no "anti-Kelvin" wave, or westward mirror image of this mode, on the dispersion diagram.

Third, the QBO of mean zonal wind is itself asymmetric as seen in Figure 2. Even if gravity wave spectra were symmetric at the tropopause, the characteristics of propagation would be different below easterly and westerly shears because of the asymmetry of the QBO. Gravity waves may partly contribute to the asymmetry of the QBO, but there are other processes, e.g., asymmetric acceleration by Kelvin and Rossby gravity waves, and the induced mean meridional circulation [*Dunkerton*, 1991].

4.2. Parameters of Possible Equatorial Waves for 1–3 Day Components

Although it was shown in section 3 that 1–3 day components are likely composed of a mixture of various waves, it would be useful to infer wave parameters of possible modes even roughly. Taking the central frequency of (1.5 days) $^{-1}$ as a typical frequency for the 1–3 day wave components, the dispersion curves are examined. As described in the following, there are at least three criteria which should be satisfied by the waves observed around the shear region.

First, from the definition of ω^* as described in section 3.5, it is found that the maximum ω^* is determined by the minimum observable vertical wavelength. Since the vertical resolution of rawinsonde observation is about 1 km, the minimum observable vertical wavelength is about 2 km (ignoring the aliasing of waves with shorter vertical wavelengths). Thus the maximum ω^* is about 4 for all equatorial wave modes.

Second, the minimum ω^* is determined by the maximum R, i.e., the ratio of PE to zonal KE, since R increases as ω^* decreases for each mode (see Figures 10a and 10b). The maximum R found from Figures 11 and 12 is 1 and 2 for westerly and easterly shear, respectively. Assuming 50% reduction due to radiative damping as discussed in section 3.5, the maximum

Table 1. Parameters of Possible Equatorial Waves for Observed 1–3 Day Components in Westerly Shear

Mode	c, m s^{-1}	λ_x, km	λ_z, km	y_0, $\times 10^3$ km
$n = -1$ Kelvin waves	>6.7	>870	>2.0	>550
$n = 1$ eastward IGW	7.7–19.6	1000–2500	2.0–4.2	550–790
$n = 3$ eastward IGW	9.4	1200	2.0	550
$n = 1$ westward IGW	−25 to −31.8	3200–4100	5.7–6.7	920–1010

The zonal phase velocity, zonal wavelength, vertical wavelength, latitudinal scale factor are denoted by c, λ_x, λ_z, and y_0, respectively. IGW, inertia-gravity waves.

R is taken to be 2 and 4 for respective shears. The minimum ω^* for each mode is denoted by open circles for westerly shear and open triangles for easterly shear in Figure 10. The thick curves in Figure 10 indicate possible waves satisfying both the first and second criteria.

Further, we can give the third criterion in terms of the mean wind. If the waves around the westerly and easterly shear come from the lower levels, their phase velocities must be out of the range of the mean wind below the shear; otherwise the waves would encounter their critical levels before reaching the shear zones. The underlying wind is about −25 to −5 m s^{-1} for westerly shear and −5 to +15 m s^{-1} for easterly shear (see Figure 2a). If we take the damping below the critical levels into account, the phase velocity range of observable waves may be more narrowed.

The possible waves satisfying these three criteria are eastward $n = -1$ modes ($c > 6.7$ m s^{-1}), eastward $n = 1$ modes ($c = 7.7$–19.6 m s^{-1}), eastward $n = 3$ modes ($c = 9.4$ m s^{-1}), and westward $n = 1$ modes ($c = -31.8$ to -25 m s^{-1}) for westerly shear. As for the easterly shear, they are eastward $n = -1$ modes ($c > 15$ m s^{-1}), eastward $n = 1$ modes ($c = 15$–44.1 m s^{-1}), eastward $n = 3$ modes ($c = 15$–20.6 m s^{-1}), westward $n = 1$ modes ($c = -61.8$ to -7.2 m s^{-1}), westward $n = 3$ modes ($c = -23.8$ to -8.6 m s^{-1}) and westward $n = 5$ modes ($c = -14.7$ to -11.7 m s^{-1}). Westward $n = 3$ modes cannot propagate through the mean wind below westerly shear, although some waves of $n = 3$ satisfy the first and second criteria. This is also the case for eastward $n = 5$ modes in the easterly shear. Parameters of the possible equatorial waves are summarized in Tables 1 and 2 for westerly and easterly shear, respectively.

The momentum flux estimated in this paper is the value at the equator. Since the QBO is a phenomena having the latitudinal half width of 25°, the latitudinal scale factor y_0 listed in Tables 1 and 2 that corresponds to the e-folding latitude of wave amplitude is important when we consider the mean wind acceleration by convergence of momentum fluxes associated with the waves. The factor y_0 is proportional to the square root of the vertical wavelength and independent of the wave frequency. The possible equatorial modes for short-period waves except for $n = -1$ modes (short-period Kelvin waves) have shorter vertical wavelengths and hence smaller meridional extent than long-period Kelvin waves with typical vertical wavelengths of 10–15 km [e.g., *Andrews et al.*, 1987] corresponding to y_0 of 940–1210 km. The possible short-period Kelvin waves have a wide range of vertical wavelengths and meridional extent which can be either larger or smaller than those of long-period Kelvin waves.

4.3. Aliasing of Waves With Periods Shorter Than 1 Day

The direct and indirect estimates of momentum flux were made under an assumption that the observed frequency is the actual ground-based frequency of the waves. Since the rawinsonde observation is made only twice a day, aliasing of waves with periods shorter than 1 day is possible. The degree of aliasing in the spectra depends on the spectral shape; blue spectra cause significant aliasing, for instance. The spectra at periods shorter than 1 day may be speculated by extrapolation of the observed spectra to higher frequencies. The cospectra in Figure 1c that were used for indirect estimate of momentum flux have larger values at shorter periods. Taking into consideration that the spectra were plotted in flux content form, the spectral shape seems nearly white. The power spectra of Figures 1a and 1b also suggest enhanced activity in 1–2 day range, which could well be due to wave motions aliased from higher frequencies. In fact, there is observational evidence of higher-frequency gravity waves associated with convection [e.g., *Sato*, 1993; *Pfister et al.*, 1993; *Sato et al.*, 1995; *Alexander and Pfister*, 1995]. The direct and indirect estimates of momentum flux are proportional to ω. The aliased higher-frequency waves can have significant momentum fluxes, although they may have smaller amplitudes than waves with periods longer than 1 day. Therefore the true values can be significantly larger than the estimates given here.

5. Summary

A new indirect method was used to estimate momentum flux from cospectra of temperature and zonal wind fluctuations based on the theory of two-dimensional (plane) gravity waves and three-dimensional equatorial waves in vertical shear [*Dunkerton*, 1995, manuscript in preparation, 1997]. This method provides the summation of absolute values of momentum flux associated with each wave. Comparing to direct estimates of total momentum flux from the quadrature spectra, we can estimate positive and negative momentum fluxes separately. An analysis was made of rawinsonde data at Singapore over 10 years. The validity of this method was reinforced by the observation of an approximately linear relationship between the cospectrum and vertical shear, and relatively few events of positive (negative) covariance of T and u components in negative (positive) vertical shear. Estimation of observational error was made to evaluate the derived momentum fluxes quantitatively.

The direct and indirect estimates for 5–20 day components in westerly shear, thought to be attributable to eastward propagating equatorial Kelvin waves, are in accord with one another to within the observational error, except for the 1987 case when Kelvin waves had such a large amplitude that we could not ignore the nonlinear effect. The direct estimates of

Table 2. Same as Table 1 but for Easterly Shear

Mode	c, m s^{-1}	λ_x, km	λ_z, km	y_0, $\times 10^3$ km
$n = -1$ Kelvin waves	>15	>1900	>2.7	>820
$n = 1$ eastward IGW	15–44.1	1900–5700	3.4–6.6	710–970
$n = 3$ eastward IGW	15–20.6	1900–2700	2.6–3.1	630–660
$n = 1$ westward IGW	−7.2 to −61.8	930–8000	2.0–9.3	550–1180
$n = 3$ westward IGW	−8.6 to −23.8	1100–3100	2.0–3.6	550–730
$n = 5$ westward IGW	−11.7 to −14.7	1500–1900	2.0–2.2	550–570

momentum flux, which are more accurate than the indirect estimates, are 2–9 $\times$ 10^{-3} m^2 s^{-2}, consistent with previous observational studies. Indirect as well as direct estimates in easterly shear are small, indicating the absence of long-period waves.

This method is effective in particular for short-period (1–3 day) disturbances because these waves can propagate both eastward and westward. The results for short-period waves are summarized as follows.

1. The indirect estimates of momentum flux under the assumption of two-dimensional gravity waves are 20–60 $\times$ 10^{-3} m^2 s^{-2} for westerly shear and 7–30 $\times$ 10^{-3} m^2 s^{-2} for easterly shear. The estimated values become smaller by about 30–70% when three-dimensional equatorial modes are assumed.

2. The direct estimates of momentum flux, which are independent of wave structure, are 0–5 $\times$ 10^{-3} m^2 s^{-2} for westerly shear and -1 to $+2$ $\times$ 10^{-3} m^2 s^{-2} for easterly shear.

3. The indirect estimates are always much larger than the direct estimates, indicating that there is a large cancelation of positive and negative momentum fluxes. If waves are mainly propagating energy upward, then eastward and westward waves must coexist, with approximately equal and opposite fluxes. It is also possible that the cancelation is partly due to reflected waves.

4. The momentum flux in one direction (approximately one-half of the total indirect estimate) is at least 3 times larger than that of long-period Kelvin waves in westerly shear.

5. There are some differences in wave characteristics between westerly and easterly shear. The ratio of potential and kinetic energy is smaller in westerly shear than in easterly shear. The indirect estimate of momentum flux, indicating wave activity, is about twice as large in westerly shear as in easterly shear.

Possible explanations for the difference between easterly and westerly shear were discussed. Wave parameters were inferred from the ratio of potential and kinetic energies and the mean wind below the shears, assuming that the short-period waves are composed of equatorial modes. The effects of aliasing, from components with periods shorter than 1 day, on the momentum flux estimation was also discussed: If there is the aliasing, the actual momentum fluxes can be significantly larger than estimated in this paper assuming that the observed frequencies are actual ground-based wave frequencies.

Singapore is located where vigorous convection is observed [e.g., *Bergman and Salby*, 1994]. The characteristics of waves near their source region may be localized, although waves in the middle and upper stratosphere possibly attain a modal, equatorially trapped structure. Further analysis is necessary using observational data at other locations near and off the equator to identify the short-period waves more precisely and to determine whether they display similar characteristics elsewhere.

Acknowledgments. The authors wish to thank Toru Sato for discussion on the estimation of observational error in the momentum flux. Thanks are extended to James R. Holton, M. Joan Alexander, and anonymous reviewers for constructive comments. This research was supported, in part by the Grant-in-Aid for Encouragement of Young Scientists (A) 07740384 of the Ministry of Education, Science and Culture, Japan (K.S.), by the National Science Foundation, grant ATM-9500613, and the National Aeronautics and Space Administration, contract NASW-4844 (T.J.D.).

References

Alexander, M. J., and L. Pfister, Gravity wave momentum flux in the lower stratosphere over convection, *Geophys. Res. Lett.*, *22*, 2029–2032, 1995.

Allen, S. J., and R. A. Vincent, Gravity wave activity in the lower atmosphere: Seasonal and latitudinal variations, *J. Geophys. Res.*, *100*, 1327–1350, 1995.

Andrews, D. G., J. R. Holton, and C. B. Leovy, *Middle Atmosphere Dynamics*, 489 pp., Academic, San Diego, Calif., 1987.

Bergman, L. W., and M. L. Salby, Equatorial wave activity derived from fluctuations in observed convection, *J. Atmos. Sci.*, *51*, 3791–3806, 1994.

Dunkerton, T. J., Nonlinear propagation of zonal winds in an atmosphere with Newtoninan cooling and equatorial wavedriving, *J. Atmos. Sci.*, *48*, 236–263, 1991.

Dunkerton, T. J., Horizontal buoyancy flux of internal gravity waves in vertical shear, *J. Meteorol. Soc. Jpn.*, *73*, 747–755, 1995.

Dunkerton, T. J., The role of gravity waves in the quasi-biennial oscillation, *J. Geophys. Res.*, this issue.

Gill, A. E., *Atmosphere-Ocean Dynamics*, 662 pp., Academic, San Diego, Calif., 1982.

Kitamura, Y., and I. Hirota, Small-scale disturbances in the lower stratosphere revealed by daily rawin sonde observations, *J. Meteorol. Soc. Jpn.*, *67*, 817–831, 1989.

Maruyama, T., Annual and QBO-synchronized variations of lower-stratospheric equatorial wave activity over Singapore during 1961–1989, *J. Meteorol. Soc. Jpn.*, *69*, 219–232, 1991.

Maruyama, T., Upward transport of westerly momentum due to disturbances of the equatorial lower stratosphere in the period range about 2 days—A Singapore data analysis for 1983–1993, *J. Meteorol. Soc. Jpn.*, *72*, 423–432, 1994.

Matsuno, T., Quasi-geostrophic motions in the equatorial area, *J. Meteorol. Soc. Jpn.*, *44*, 25–43, 1966.

Ogino, S., M. D. Yamanaka, and S. Fukao, Meridional variation of lower stratospheric gravity wave activity: A quick look at Hakuho-Maru J-COARE cruise rawinsonde data, *J. Meteorol. Soc. Jpn.*, *73*, 407–413, 1995.

Pfister, L., K. R. Chan, T. P. Bui, S. Bowen, M. Legg, B. Gary, K. Kelly, M. Proffitt, and W. Starr, Gravity waves generated by a tropical cyclone during the STEP tropical field program: A case study, *J. Geophys. Res.*, *98*, 8611–8638, 1993.

Sato, K., Small-scale wind disturbances observed by the MU radar during the passage of Typhoon Kelly, *J. Atmos. Sci.*, *50*, 518–537, 1993.

Sato, K., F. Hasegawa, and I. Hirota, Short-period disturbances in the equatorial lower stratosphere, *J. Meteorol. Soc. Jpn.*, *72*, 423–432, 1994.

Sato, K., H. Hashiguchi, and S. Fukao, Gravity waves and turbulence associated with cumulus convection observed with the UHF/VHF clear-air Doppler radars, *J. Geophys. Res.*, *100*, 7111–7119, 1995.

Takayabu, Y. N., K.-M. Lau, and C.-H. Sui, Observation of quasi two-day wave during TOGA COARE, *Mon. Weather Rev.*, *124*, 1892–1913, 1996.

Tsuda, T., Y. Murayama, H. Wiryosumarto, S. W. B. Harijono, and S. Kato, Radiosonde observations of equatorial atmosphere dynamics over Indonesia, 1, Equatorial waves and diurnal tides, *J. Geophys. Res.*, *99*, 10,491–10,506, 1994a.

Tsuda, T., Y. Murayama, H. Wiryosumarto, S. W. B. Harijono, and S. Kato, Radiosonde observations of equatorial atmosphere dynamics over Indonesia, 2, Characteristics of gravity waves, *J. Geophys. Res.*, *99*, 10,507–10,516, 1994b.

T. J. Dunkerton, Northwest Research Associates, P.O. Box 3027, Bellevue, WA 98009. (e-mail: tim@nwra.com)

K. Sato, Department of Geophysics, Kyoto University, Kyoto 606-01, Japan. (e-mail: sato@kugi.kyoto-u.ac.jp)

(Received April 9, 1996; revised July 31, 1996;
accepted July 31, 1996.)